

RECENT IMPROVEMENTS TO THE CONTROL OF THE CTF3 HIGH-CURRENT DRIVE BEAM

B. Constance, R. Corsini, D. Gamba, P. K. Skowroński, CERN, Geneva, Switzerland

Abstract

In order to demonstrate the feasibility of the CLIC multi-TeV linear collider option, the drive beam complex at the CLIC Test Facility (CTF3) at CERN is providing high-current electron pulses for a number of related experiments. By means of a system of electron pulse compression and bunch frequency multiplication, a fully loaded, 120 MeV linac is used to generate 140 ns electron pulses of around 28 Amperes. Subsequent deceleration of this high-current drive beam demonstrates principles behind the CLIC acceleration scheme, and produces 12 GHz RF power for experimental purposes. As the facility has progressed toward routine operation, a number of studies aimed at improving the drive beam performance have been carried out. Additional feedbacks, automated steering programs, and improved control of optics and dispersion have contributed to a more stable, reproducible drive beam with consequent benefits for the experiments.

INTRODUCTION

The Compact Linear Collider [1] (CLIC) is a leading contender for the next generation of high energy lepton colliders. As an essential precursor to proceeding with such a facility, the CLIC Test Facility (CTF3) at CERN has been built to demonstrate many of the technologies required for stable drive beam generation and RF power production. The complex consists of a 120 MeV e^- linac, a chicane for bunch length control, a 42 m Delay Loop (DL), an 84 m Combiner Ring (CR) and finally the CLIC Experimental Area (CLEX). A thermionic gun produces 4 Amp pulses of 1.4 us, typically at a repetition rate of 0.83 or 1.67 Hz. A sub-harmonic buncher operating at 1.5 GHz, followed by a 3 GHz buncher, generates a beam bunched at half the acceleration frequency. Since energy efficiency is key to the CLIC design, the 3 GHz CTF3 linac operates in a fully loaded configuration. In order to maximise the RF power available, 5.5 us pulses from the klystrons are compressed to around 1.4 us using resonant cavities, increasing peak power by a factor of two to over 30 MW.

As laid out in the CLIC design, at CTF3 a system of bunch frequency multiplication and pulse compression is used to generate a high-current drive beam. Injection into the DL and CR is achieved using transverse deflecting RF cavities. By coding the beam phase with a series of 180° phase shifts, 140 ns sections of the pulse may be alternately injected or allowed to bypass the DL. On exiting the DL, the delayed sections interleave with those sections bypassing. This results in a train of four 140 ns sub-pulses, sep-

arated by 140 ns, with a current of some 8 Amps and a 3 GHz bunch frequency. These four sub-pulses are then stacked in the CR before extraction to CLEX, where the final 12 GHz pulse is 140 ns long. The combined current is typically around 28 Amps before transport, since some fraction of the charge is lost to satellite bunches in the unused RF buckets.

In CLEX, the combined pulse may be directed to one of two experimental beamlines. The Test Beam Line (TBL) contains at present 12 Power Extraction and Transfer Structures (PETS), with 16 expected by end of the 2012, and is used primarily for studies into the phase and amplitude stability of the produced 12 GHz RF power and the transport of the decelerated drive beam [2]. The second beamline serves the Two-Beam Test Stand (TBTS), an experiment which is also provided a probe e^- beam by the CALIFES accelerator. The probe beam fills the role of the CLIC main beam, allowing for two-beam acceleration studies [3].

OPTICAL MODEL VERIFICATION

Control of the transverse linear optics at CTF3 is achieved using a MAD-X model of the machine. Optical transition radiation screens at key points in the lattice allow measurements of the beam emittance and Twiss parameters using standard quadrupole scan techniques. Based on these measurements, quadrupole currents are rematched using the model predictions to ensure the correct beam parameters at critical locations. Of course, the success of this method depends on the validity of the model.

Discrepancies between the predicted and measured optical functions at some screens inspired a campaign to verify the MAD-X model using beam-based optics measurements. The horizontal and vertical planes were assumed to be uncoupled and treated independently. Using a pair of calibrated dipole corrector magnets separated by a drift length, a series of beam orbits may be injected into the lattice with arbitrary positions and angles. The series of orbits can be chosen in such a way that they map out, or paint, the matched phase space ellipse expected at the location of the second corrector. In effect, each orbit behaves as a macroparticle on the matched ellipse. The orbits evolve as they propagate through the lattice in a way governed by the linear transport matrix, and thus so too does the ellipse they describe. By spacing the orbits at regular intervals covering the full phase space, and observing how the ellipse has changed at some downstream position, information is obtained about all four elements of the two-dimensional transfer matrix.

To reconstruct the ellipse at a downstream point requires a measurement of both the position and angle at this point. At CTF3, the Beam Position Monitors (BPMs) available give only position information, and therefore measurements from two adjacent BPMs are combined to calculate the orbit angles. For this step it is necessary to assume the MAD-X model between the two BPMs is correct.

For practical measurements, it is advantageous to take pairs of orbits on the ellipse separated by a 180° phase advance and use them to form a difference orbit. In this way slow drifts of the beam will be canceled. In addition, mean difference orbits over a number of pulses may be taken. To further reduce sensitivity to jitter and drifts, several similar ellipses of different areas or pseudo-emittances may be painted. Then, a fit can be made between the difference orbits at a given phase over all ellipses and a single, normalised ellipse generated.

To extract the transfer matrix from an ellipse reconstructed at some point s in the lattice, each set of N orbits is formed into a matrix $\mathbf{x}(s)$:

$$\mathbf{x}(s) = \begin{pmatrix} x_1(s), & x_2(s), & \dots & x_N(s) \\ x'_1(s), & x'_2(s), & \dots & x'_N(s) \end{pmatrix} \quad (1)$$

Then, letting s_B denote the location of the reconstruction BPM and s_K the location of the kicker:

$$\mathbf{x}(s_B) - \mathbf{M}\mathbf{x}(s_K) = 0 \quad (2)$$

Which may be solved numerically for the transfer matrix \mathbf{M} . Here, the equation was solved using a non-linear fitting routine implemented in MATLAB [4] with the symplectic constraint imposed in addition.

As reconstruction of the ellipse requires an assumption of the transfer matrix between BPMs, it is necessary to require consistency over multiple measurements to be certain of a measured transfer matrix's veracity. Take the situation in figure 1. In the first step, matrix \mathbf{M}_1 is measured assuming \mathbf{N}_1 to be correct. In the second step, \mathbf{M}_2 is measured assuming \mathbf{N}_2 . If both \mathbf{M}_1 and \mathbf{M}_2 are consistent with MAD-X, then since $\mathbf{M}_2 = \mathbf{N}_1\mathbf{M}_1$ the original assumption of \mathbf{N}_1 is upheld. It is possible to proceed pairwise through all BPMs in the lattice in this manner.

After making measurements of various sections of CTF3, the MAD-X model was found to accurately represent the lattice in most cases. One notable exception was

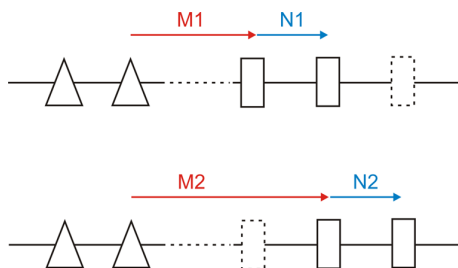


Figure 1: Procedure for measurement of the transfer matrix \mathbf{M}_1 between the second corrector magnet and first BPM.

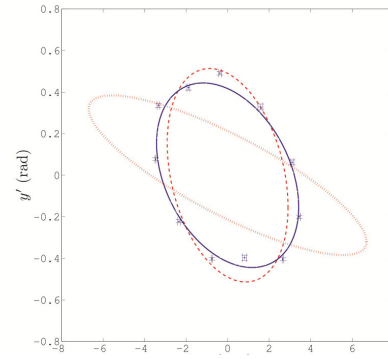


Figure 2: Reconstructed vertical ellipse at the DL BPM named BPI0358. Data points show the difference orbits. The solid blue ellipse is generated by the symplectic fit to the data, and is compared to the MAD-X prediction before (dotted red) and after (dashed red) optimisation of the main dipole FINT property.

the DL, where good agreement was obtained in the horizontal but a discrepancy was clear in the vertical. This suggested an error in the modeling of the main dipole fringe fields. By using an iterative procedure again developed in MATLAB, it was possible to fit the dipole field integral (FINT property in MAD-X) to provide the best possible match with the measurements. At each step in the iteration, the new model matrices must of course be used to reconstruct the ellipses.

In figure 2 an example of a reconstructed ellipse is shown, along with the MAD-X prediction before and after optimising the field integral. Figure 3 shows the four measured matrix elements throughout the DL lattice, again with the MAD-X predictions. In addition, a direct measurement of R_{11} and R_{12} was made by injecting a cosine- and sine-like orbit respectively, and is included for comparison. The missing measurements in the centre of the DL are due to faulty BPMs, and the matrices are given with respect to the DL injection point.

ONLINE DISPERSION MEASUREMENT

By taking advantage of CTF3's RF pulse compression system, a simple method to monitor dispersion during tuning is in use. A programmed phase ramp ensures a flat top to the compressed RF pulses. By appropriate modification of the phase ramp, a step in the RF may be introduced such that the second half of the pulse has around 2 MW ($\sim 10\%$) lower power than the first half. During tuning, this is done with the RF from the klystron that drives the final two cavities. Online orbit display software is then used to display the mean orbits of the first and second half of the beam pulse, along with a difference between the two. This difference is proportional to the dispersion function.

In figure 4, the orbits of the beginning and end of the pulse are shown along the linac, bypassing the DL and in the TL1 transfer line leading toward the CR, as is the difference between them. In the second plot a quadrupole in the

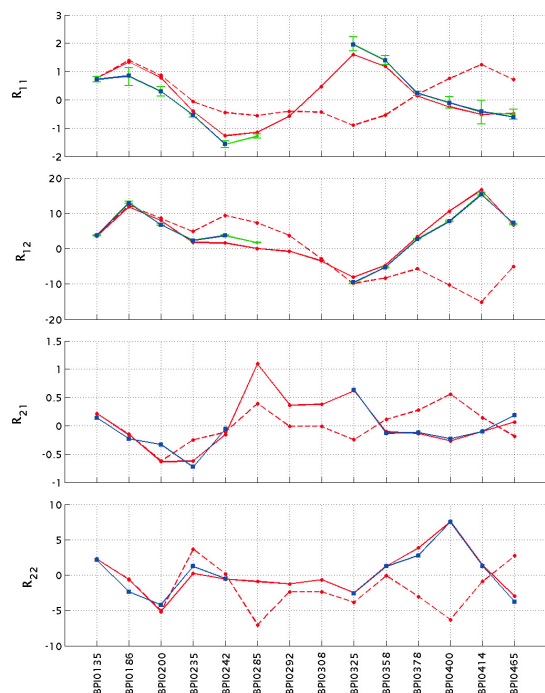


Figure 3: Vertical transport matrices for the DL. Matrices from MAD-X before (dashed red circles) and after (solid red circles) optimisation of the main dipole FINT are compared with the measured matrices extracted from reconstructed ellipses (solid blue squares) and direct measurements of R_{11} and R_{12} (green error bars).

dispersive region of the chicane, between the BPMs 0242 and 0258, has been used to minimise the downstream dispersion.

AUTOMATIC ORBIT CLOSURE

Closure of the CR orbit and of the orbit exiting the DL are very important to the generation of a well-combined beam, since different sub-pulses of the beam take different paths through the machine and are stored in the CR for different numbers of turns. To aid in operation, automatic

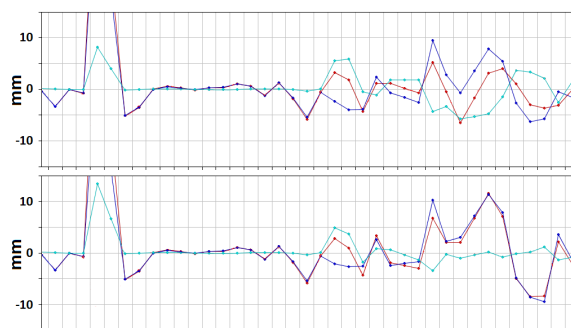


Figure 4: Horizontal orbit in the linac and TL1 before (top) and after (bottom) dispersion correction. The blue and red orbits have high and low energy respectively, and cyan shows the difference between the two.

ISBN 978-3-95450-122-9

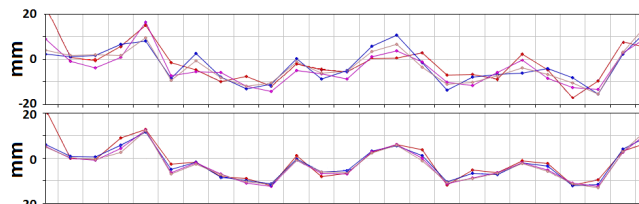


Figure 5: Horizontal orbit in the CR before (top) and after (bottom) automatic steering to inject onto the closed orbit. Each trace shows one of the four turns.

software has been developed to steer the beam in the DL out onto the same trajectory as the bypassing sub-pulses. Similarly, software is used to steer the beam onto the closed orbit of the CR. Based on measured response matrices, the system is automatic and can operate as a slow feedback to counter beam drift.

In figure 5, the horizontal orbits of four turns in the CR are shown. The 4 Amp pulse has been shortened to prevent combination. The second plot shows the effects of automatically steering the beam onto the closed orbit, which had previously been found by storing the beam for around ten turns and allowing the orbit oscillations to damp. The apparent residual difference between the turns in some BPMs is an artifact due to a droop of the BPM signal baselines. Well behaved BPMs such as 0650 and 0695 show the true orbit difference.

CONCLUSION

Beam-based measurements of the linear optics have been performed, and an error in the MAD-X model of the DL corrected. Ensuring the delayed sub-pulses and sub-pulses which bypass the DL are optically matched leads to easier transport of the combined pulse. The use of online dispersion monitoring and automatic steering has allowed for a faster and more precise setup of the beam, improving reproducibility. Coupled with recent improvements in dynamic control of CTF3, such as feedbacks which have improved the stability of the compressed RF pulses [5, 6], these developments have led to a more stable environment for research.

REFERENCES

- [1] G. Guignard (Ed.), "A 3 TeV e+e- linear collider based on CLIC technology," CERN 2000-008, 2000.
- [2] E. Adli et al., "Commissioning status of the decelerator test beam line in CTF3," MOP018, LINAC2010.
- [3] W. Farabolini et al., "Two beam test stand experiments in the CLEX CTF3 facility," MOOCA02, IPAC2011.
- [4] MathWorks, <http://www.mathworks.com/>
- [5] A. Dubrovskiy and F. Tecker, "RF pulse compression stabilization at the CTF3 CLIC test facility," THPEA043, IPAC2010.
- [6] T. Persson and P. K. Skowronski, "Beam stability at CTF3," TUPPR032, IPAC2012.